Magazine of Civil Engineering

ISSN 2712-8172

journal homepage: http://engstroy.spbstu.ru/

Research article

UDC 534.1

DOI: 10.34910/MCE.134.3

Analysis of rheological model parameters for various foamed vibration-damping materials

M.V. Shitikova ✉ , ***V.A. Smirnov***

Moscow State University of Civil Engineering (National Research University), Moscow, Russian Federation

✉ *shitikova@vmail.ru*

Keywords: viscoelastic materials, fractional derivatives, resonance testing, dynamic modulus, loss factor, material density, pore structure, polyurethane foam, damping properties, rheological modeling

Abstract. The study presents an experimental and analytical investigation of foamed polyurethane viscoelastic materials with varying density and pore structures, focusing on their dynamic mechanical behavior relevant for vibration damping applications. Samples with distinct pore configurations (open, closed, and combined) and varying densities (165–380 kg/m^3) were subjected to resonance-based dynamic tests under static loads of 2, 5, and 10 kPa. The dynamic modulus of elasticity and damping characteristics, including loss factor, fractional damping parameters, and relaxation times, were determined. Results indicated that damping properties are strongly influenced by material density and internal pore structure, with closed-pore materials exhibiting lower damping capacities compared to materials with open or combined pores. A Fractional Standard Linear Solid (FSLS) model was effectively utilized to characterize the observed nonlinear viscoelastic behaviors, successfully correlating experimental data through parameter identification methods. The findings confirm that increased density generally enhances the dynamic modulus while reducing damping capacity, whereas pore structure significantly affects the material's dynamic response. These insights validate fractional derivative models as efficient predictive tools, facilitating the optimized design of viscoelastic isolation systems for engineering structures.

Funding: This research has been supported by the Ministry of Science and High Education of the Russian Federation, Project No.07-03-2023-132 (FZGM-2023-0006).

Citation: Shitikova, M.V., Smirnov, V.A. Analysis of rheological model parameters for various foamed vibration-damping materials. Magazine of Civil Engineering. 2025. 18(2). Article no. 13403. DOI: 10.34910/MCE.134.3

1. Introduction

Viscoelastic materials have been widely employed in numerous branches of science and engineering to address critical issues such as reducing dynamic impacts on supporting structures, vibration and seismic isolation of buildings and technical systems, and modifying the dynamic stiffness of structural elements. In these applications, understanding the dynamic behavior of the viscoelastic elements is indispensable for ensuring the reliability and efficiency of isolation and damping systems. Such behavior is inherently rate-dependent, as the stiffness and damping characteristics of elastomers and polymeric foams generally exhibit considerable sensitivity to strain rate, frequency, and amplitude of excitation. Consequently, formulating accurate constitutive models becomes pivotal in designing vibration and seismic isolation systems with predictable performance over their entire service life.

A broad spectrum of rheological models has been proposed to capture the complex time- and frequency-dependent behavior of viscoelastic materials, ranging from simple two-parameter models, such as the Kelvin–Voigt or Maxwell models, to sophisticated multi-element generalized models containing

multiple chains of springs and dashpots [1]. However, classical integer-order models can fail to capture certain real-world behaviors, especially when damping mechanisms arise from multiple or overlapping relaxation processes. Furthermore, simplified models sometimes yield unphysical predictions. For instance, Kelvin–Voigt-type models may exhibit artificially high or even unbounded loss factors under specific parametric conditions. On the other hand, highly parameterized multi-element frameworks, such as the Mooney–Rivlin model with eleven or more parameters, demand extensive experimental campaigns, making them impractical for many engineering contexts.

Recent studies emphasize that these challenges can often be addressed by leveraging fractional calculus, which introduces fractional-order derivatives into standard viscoelastic models. Fractional operators enable more flexible representation of material memory effects than their integer-order counterparts [2, 3]. Such models, including the Fractional Kelvin–Voigt, Fractional Maxwell, and Fractional Standard Linear Solid (FSLS) models, can reconcile high modeling accuracy with comparatively fewer model parameters [4]. Moreover, numerical advancements in solving fractional differential equations [5] further encourage the use of fractional derivatives in practical applications.

Early applications of fractional viscoelastic models in structural mechanics have demonstrated promising results. Studies on beams, plates, and shells resting on fractional viscoelastic foundations [6–9] have shown that incorporating fractional damping provides excellent agreement between experimental data and theoretical predictions for a wide range of frequencies. Furthermore, fractional operator models have found utility in seismology, where they can represent constant-Q (quality factor) seismic waves more effectively than classical integer-order approaches [10, 11]. These successes align with other experimental validations in the literature: for instance, fractional models have demonstrated high fidelity in capturing the creep and recovery behavior of asphalt mixtures [12], the rheological response of fiber-reinforced rubber concrete [13], large-amplitude vibrations in metallic and polymeric systems [14], and viscoelasticity in polyethylene [15, 16], silicone [17, 18], and various rubber compounds [19].

Notably, fractional derivative-based methodologies have facilitated accurate and efficient identification of viscoelastic parameters. Beda and Chevalier [20] proposed a parametric identification technique to determine fractional exponents and relaxation moduli from limited experimental datasets. Similarly, Espíndola et al. [21] and Guo et al. [22] extended these approaches to thermoplastics and polymeric acoustic foams, revealing that fractional damping parameters often remain within a relatively narrow range under typical operational conditions, thus enabling simpler yet robust models. In these studies, the deviation between model predictions and experimental data was reported to be significantly lower compared to classical models – often below 5 % across a wide frequency range.

Despite the recognized advantages, an ongoing challenge in fractional derivative modeling pertains to the identification of fractional parameters from experimental data, which can be especially sensitive to measurement noise, excitation frequencies, and other test conditions [5]. Recent investigations [13] demonstrated that the fractional exponent for fiber-reinforced rubber concrete could be identified by comparing analytical solutions of the FSLS model with experimental resonance data, obtaining an excellent agreement (errors consistently under 4 % in the measured stiffness loss). Similar conclusions were made for other polymeric and hyperelastic materials, highlighting how fractional damping exponents effectively characterize time-dependent material behavior in both the low- and high-frequency regimes [17, 18, 20–22].

Driven by these findings, the present study focuses on foamed polyurethane vibration-damping materials with combined pore structures and varying densities, aiming to elucidate the role of fractional parameters in their dynamic response. By performing a series of resonance tests, the mechanical properties – dynamic modulus of elasticity and loss factor – are obtained under a range of static preloads and dynamic excitations. These datasets serve as inputs to a FSLS model, whose parameters are systematically identified via nonlinear least squares optimization. Emphasis is placed on capturing both stiffness and damping variations across different densities and pore structures, thereby highlighting the nuanced influence of foam microstructure on global vibrational performance.

This paper presents a comprehensive experimental and analytical framework – encompassing test setup, data acquisition, and model parameter identification – to ensure reliable quantification of viscoelastic behavior. The insights gained herein extend the applicability of fractional operator modeling to a broader class of vibration-damping materials, contributing to advanced design strategies for high-efficiency passive isolation and noise control systems. The following sections detail the experimental methodology, describe the fractional-derivative-based approach to parameter identification, and discuss the implications of the results for future research and practical applications in vibration and seismic isolation.

2. Method

2.1. Materials with Different Stiffness

Let us first consider the behavior of vibration-damping materials, widely used in various fields of engineering and construction, made on the basis of foamed polyurethanes with different combination of closed and open pores, as well as with different densities.

For a comparative evaluation of the behavior of materials under dynamic impact a series of samples (type s.1.1–s.1.4 in Fig. 1 a–d) with combined pore structure and increasing density, as well as materials with approximately the same density but different structure: type s.2.1 with closed pores (Fig. 1 e) and type s.1.4 (Fig. 1 d) are considered.

These materials, due to their foam structure, have pronounced nonlinear characteristics. When the applied compression load increases, the stiffness of the material in the range of its operation decreases, which is due to the structural features of "collapse" of open pores and "pumping" of sealed air, and, having reached the limit value, begins to increase.

The internal structure of the samples (slice fixation) of the materials is shown in Fig. 1. The images were obtained using an optical microscope with 50x – 100x magnification. For materials of types s.1.1–s.1.4 it could be noted that the increase in density occurs with a simultaneous increase in the number of internal pores and a decrease in their size – the spread between large and small pores decreases and their total diameter becomes more and more constant.

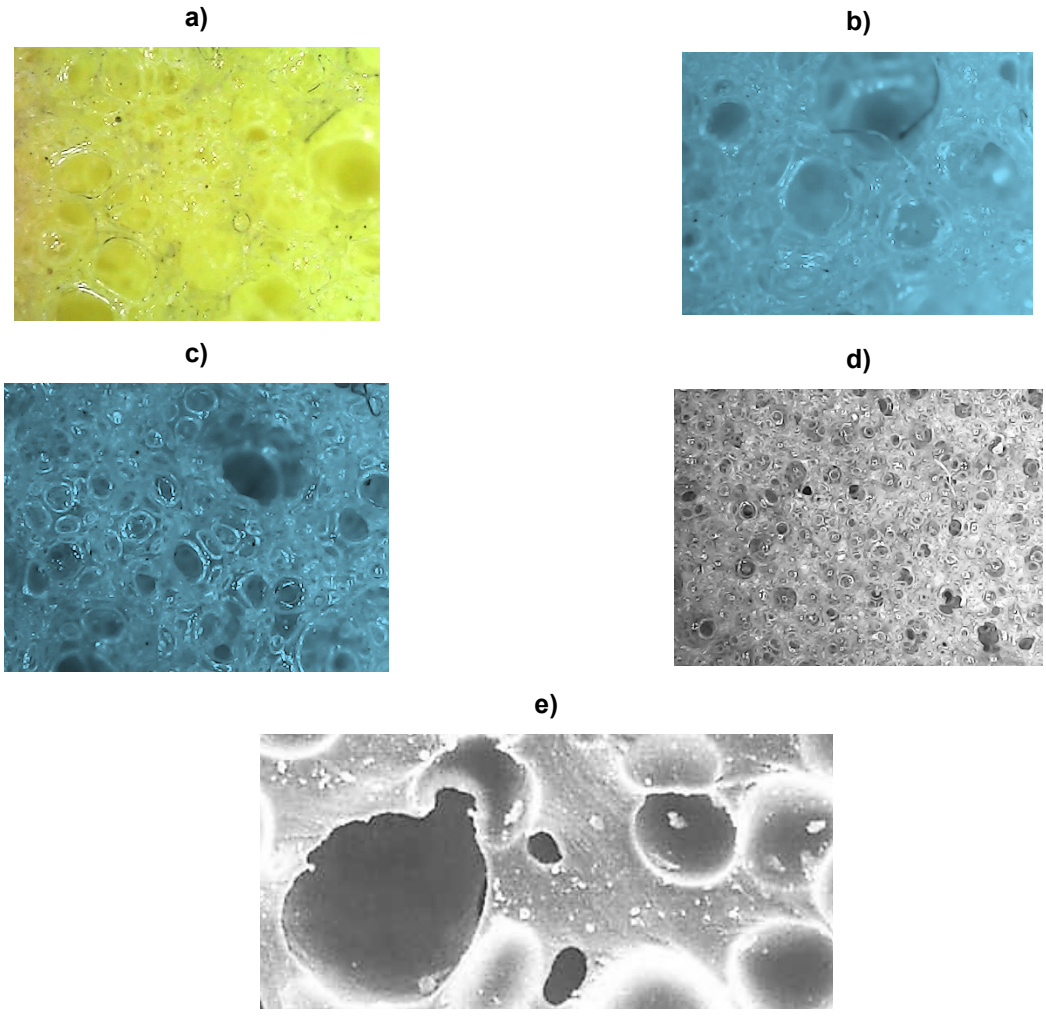

Figure 1. Internal porous structure f material samples: a) type s.1.1; b) type s.1.2; c) type s.1.3; d) type s.1.4; e) type s.2.1.

2.2. Materials with Different Damping

We also consider the behavior of vibration-damping materials based on polyurethane foam, used as a vibration-damping layer of vibration isolation systems for buildings and structures, machine foundations and high-precision equipment.

Two series of materials of approximately the same stiffness but with different structural features are considered for comparative evaluation of materials behavior under dynamic influence:

- type d.1 – material with closed pores, which has the most elastic properties;
- type d.2 – material with communicating pores, it has high damping, its properties are close to those of viscous liquids;
- type d.3 – material with combined pore structure, it combines the properties of materials of types d.1 and d.2.

These materials, due to their foamed structure, have pronounced nonlinear characteristics. When the applied compression load increases, the stiffness of the material in the range of its operation decreases, which is due to the structural features of "collapse" of open pores and "pumping" of sealed air, and, having reached the limit value, begins to increase.

2.3. Experimental Method

To determine the mechanical characteristics of the materials under study, a series of dynamic tests were carried out using the resonance method on a stand developed in accordance with GOST 16297-80, the general scheme of which is shown in Fig. 2. Experimental studies were carried out for samples in the form of square plates with dimensions of 100 × 100 × 25 mm. The sample of vibration-damping material 3 was installed on the stage 2 of electrodynamic vibro-exciter 1 and loaded with steel cylinders (masses) 4, providing constant loads on the sample of 2, 5 and 10 kPa.

Tests were conducted when the sample was subjected to broadband (white) noise. The perturbation signal was set by the oscillation generator RFT 03004 7, which through the amplifier RFT LV-102 8 was connected to the vibration exciter ESE-201 type 1. During the tests, the accelerations of the moving part of the electrodynamic vibration exciter (base) 5' – function $z(t)$, as well as the response of the system 5 – function $x(t)$ were recorded by single-axis accelerometers PCB and multichannel measuring system LCARD LTR-24-2.

a) **b)**

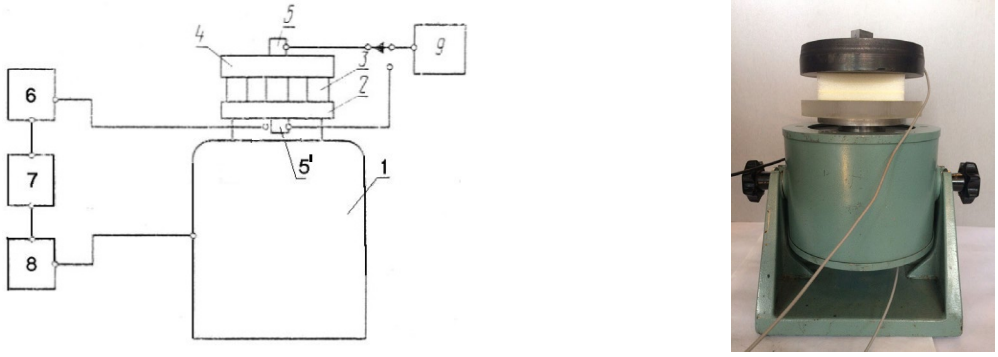

Figure 2. Test bench for dynamic tests by resonance method:
a) schematic diagram of the test bench; b) photo of the shaker.

According to the results of dynamic tests by the resonance method, the measured accelerograms of base vibration $\ddot{z}(t)$ and mass $\ddot{x}(t)$ were processed to obtain the spectral characteristics of $\ddot{z}(\omega)$ and $\ddot{x}(\omega)$. The transfer function $\mathrm{Tr}(\omega)$ is defined as the ratio of the spectral characteristics of the vibration accelerations obtained at the mass to the spectral characteristics of the vibration accelerations recorded at the base:

$$\mathrm{Tr}(\omega)=\left|\frac{\ddot{x}(\omega)}{\ddot{z}(\omega)}\right|, \tag{1}$$

where ω is the frequency of external kinematic influence, Hz.

Fig. 3 shows experimentally obtained curves of the transfer function modulus $\mathrm{Tr}(\omega)$ for the object of study in the frequency range of 1–500 Hz at a constant load on the sample of 5 kPa.

Note that for materials with combined pores of types s.1.1–s.1.4, shown by the dashed line, with increasing density, an increase in the resonance frequency of oscillations from 26 Hz (for type s.1.1) to

53 Hz (for type s.1.4) is observed. At the same time, the amplitude of the transfer function modulus at the resonance frequency remains approximately constant and varies in the range of 3–4. The materials of types s.1.4 and s.2.1, having comparable density but different structure, show differences in the region of the resonance frequency of the system: the material with closed pores (type s.2.1) has a lower resonance frequency (44 Hz vs. 53 Hz) and a much larger (3 times) amplitude of the resonance peak.

The dynamic modulus of elasticity of the material could be determined in accordance with GOST 16297-80 using the formula:

$$E_{dyn} = \frac{4\pi^2 \omega_0^2 Ml}{S}, \tag{2}$$

where ω_0 is the resonant frequency of the system, Hz; M is the mass of the load, kg; l is the height (thickness) of the sample under load, m; and S is the area of the tested sample, m^2.

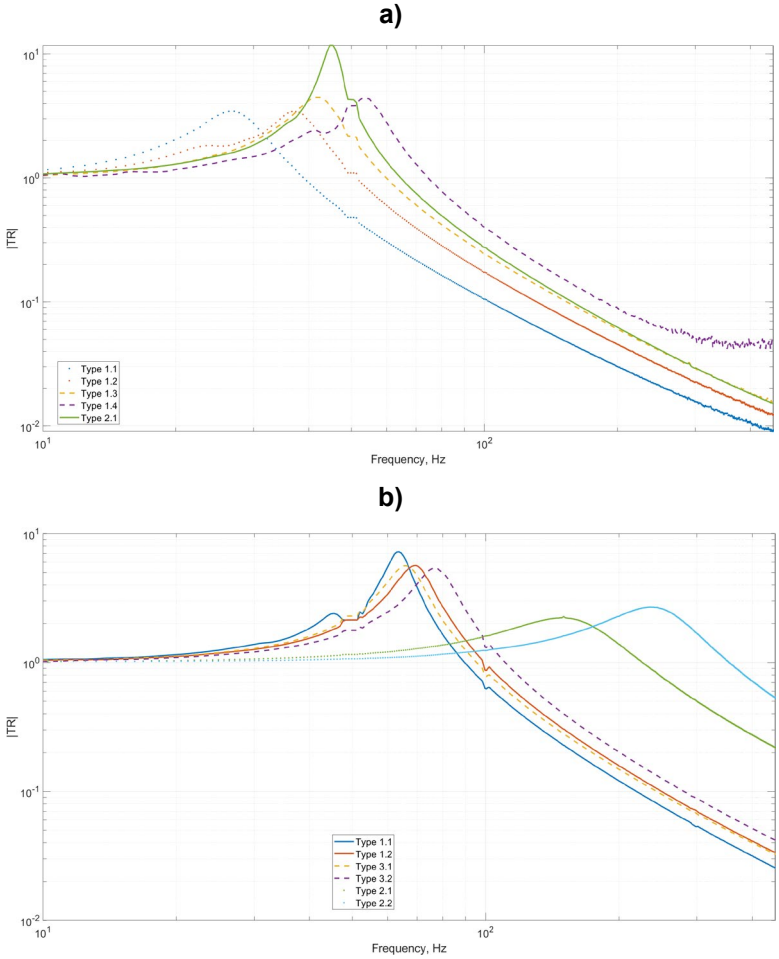

Figure 3. Modulus curves of the transfer function for the considered materials at a constant load of 5 kPa: a) for materials with different stiffness, and b) for materials with different damping.

The resonant frequency has been determined as the frequency corresponding to the maximum peak on the transfer function graph.

The loss factor has been evaluated by the width of the resonance peak [23], as shown in Fig. 4. In this case, points A and B on the graph correspond to the frequencies at which the amplitude of accelerations is $\sqrt{2}$ times smaller than the maximum amplitude achieved at the resonant frequency.

Considering the introduced notations, the formula for the loss factor will be as follows:

$$\eta = \frac{\omega_2 - \omega_1}{\omega_0}. \tag{3}$$

Table 1 shows the obtained mechanical characteristics of the investigated materials.

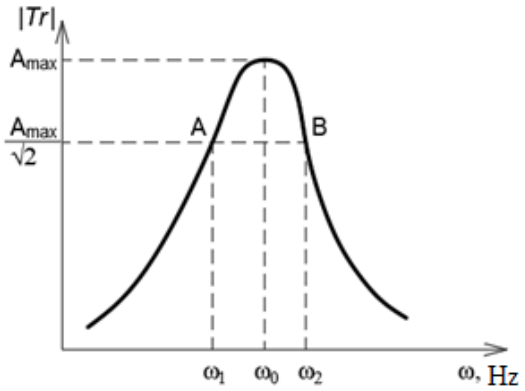

Figure 4. Schematic of resonance peak width determination.

Table 1. Dynamic parameters of the object of study.

Material identification		Density, kg/m³	Load, kPa	E_{dyn}, MPa	η
Materials with different stiffness	Type s.1.1	165	2	0.428	0.440
			5	0.333	0.420
			10	0.179	0.670
	Type s.1.2	190	2	0.657	0.299
			5	0.659	0.324
			10	0.572	0.600
	Type s.1.3	210	2	0.637	0.423
			5	0.846	0.281
			10	0.782	0.343
	Type s.1.4	380	2	1.129	0.250
			5	1.275	0.237
			10	1.176	0.399
	Type s.2.1	350	2	0.909	0.172
			5	0.969	0.155
			10	0.952	0.192
Materials with different damping	Type d.1.1	343	2	0.788	0.221
			5	1.000	0.130
			10	1.050	0.079
	Type d.1.2	467	2	0.827	0.402
			5	1.190	0.187
			10	1.450	0.164
	Type d.2.1	353	2	3.070	0.664
			5	5.560	0.600
			10	6.690	0.620
	Type d.2.2	572	2	7.280	0.581
			5	13.640	0.483
			10	16.150	0.491
	Type d.3.1	280	2	0.724	0.288
			5	1.070	0.194
			10	1.260	0.177
	Type d.3.2	381	2	1.060	0.319
			5	1.459	0.198
			10	1.650	0.148

Materials belonging to type s.1 & d.1 have a combination of open and closed pores and have pronounced viscoelastic properties with a relatively small loss factor value. It can be noted that with increasing density, the dynamic modulus of elasticity increases, and the loss factor decreases. Materials

with a structure with closed pores (type s.2.1) have more pronounced elastic properties, as evidenced by rather low values of the loss factor compared to other samples.

2.4. Rheological Material Models

For mathematical description of viscoelastic characteristics of the considered materials, we would adopt the standard linear solid model with fractional derivative, the rheological model of which is presented in Fig. 5 in two modifications: Zener–Rzhanitsyn (Fig. 5 a) and Poyting–Thomson–Ishlinsky (Fig. 5 b). Both variants are described by the following equation [3]:

$$\sigma + \tau_{\varepsilon}^{\gamma} D^{\gamma}\sigma = E_0\left(\varepsilon + \tau_{\sigma}^{\gamma} D^{\gamma}\sigma\right), \tag{4}$$

where σ is the stress in the element, N/mm^2; ε is the strain of the viscoelastic element; τ_σ and τ_ε are the creep and relaxation times, respectively, s; E_0 and E_∞ are the relaxed and instantaneous elastic moduli, respectively, N/mm^2.

The fractional derivative in the Riemann–Liouville representation is defined as

$$D^{\gamma}x(t) = \frac{d}{dt}\int_0^t \frac{x(t-u)\,du}{\Gamma(1-\gamma)u^{\gamma}}, \tag{5}$$

where $\Gamma(1-\gamma)$ is the Gamma-function.

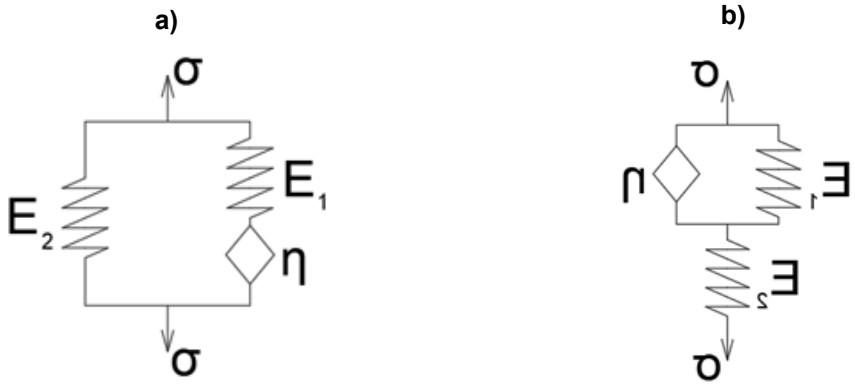

Figure 5. Standard linear solid model: a) Zener–Rzhanitsyn representation, and b) Poyting–Thomson–Ishlinsky representation.

Further we will use the standard linear solid model in the Zener–Rzhanitsyn representation, consisting of an elastic element with modulus E_2, N/mm^2, connected in parallel with a fractional analog of a Maxwell element involving an elastic element with modulus E_1, N/mm^2, and a viscous element η.

Parameters of this model entering in equation (4) are described by the following relationships [3]:

$$E_0 = E_2, \quad E_\infty = \frac{E_1 E_2}{E_1 + E_2},$$

$$\tau_{\varepsilon}^{\gamma} = \frac{\eta}{E_1}, \quad \tau_{\sigma}^{\gamma} = \frac{E_1 + E_2}{E_1 E_2}\eta, \quad \left(\frac{\tau_\varepsilon}{\tau_\sigma}\right)^{\gamma} = \frac{E_0}{E_\infty}. \tag{6}$$

Let us consider the mechanical model corresponding to the experimental studies performed in Section 2.

The relationship between the stiffness parameters k_1, k_2 and viscosity coefficient c of the mechanical model (Fig. 6) and the rheological model parameters E_1, E_2 and η (Fig. 5 a) is the following:

$$k_1 = \frac{S}{l}E_1, \quad k_2 = \frac{S}{l}E_2, \quad c = \frac{S}{l}\eta, \tag{7}$$

where S and l are the area and height (thickness) of the rectangular material specimen under load.

In this case, the damper will be described by the relation $c = \tau_\varepsilon^\gamma k_1$, where γ is the fractional parameter $(0 \le \gamma \le 1)$. When $\gamma \to 0$, the material has purely elastic behavior, and when $\gamma \to 1$, it has purely viscous behavior. In fact, every material has some combination of elastic and viscous properties.

The transfer function (1) for a single-mass system with a viscoelastic element described by equation (4), in the case of a kinematic perturbation of the base $\ddot{z}(t) = \ddot{Z}_0 e^{i\omega t}$ will take the following form:

$$\mathrm{Tr}_{sls} = \frac{\ddot{x}}{\ddot{z}} = \frac{1 + (N\tau_\varepsilon)^\gamma (i\omega)^\gamma}{1 + (N\tau_\varepsilon)^\gamma (i\omega)^\gamma - \left(\frac{\omega}{\omega_0}\right)^2 \left(1 + \tau_\varepsilon^\gamma (i\omega)^\gamma\right)}, \tag{8}$$

where $\omega_0 = \sqrt{\frac{k}{m}}$, $i = \sqrt{-1}$, $N = \frac{\tau_\sigma}{\tau_\varepsilon}$.

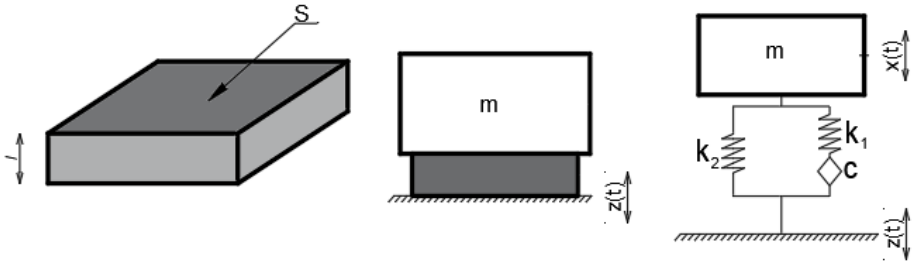

Figure 6. Single-mass oscillating system with a viscoelastic foundation.

3. Results and Discussion

To describe the material behavior by the standard linear solid model with fractional derivative, it is necessary to know 5 parameters: E_0, E_∞, τ_ε, τ_σ, γ, in so doing 4 of them to be determined, and the 5th one could be obtained using relations (6).

The experimentally obtained transfer functions $\mathrm{Tr}(\omega)$ (1) was approximated by the curve described by the analytical solution (8) for the oscillating system shown in Fig. 6. The optimization problem was solved in the MATLAB program Optimization Toolbox by the nonlinear least squares method using the *lsqcurvefit* function. The natural frequency ω_0 obtained from the experimental results was set as an initial approximation.

Fig. 7 shows a graphical representation of the result of approximation of the experimental data for material type 2.1 at a load of 2 kPa. Dots indicate experimental data, solid red line refers to the approximated curve, red dotted line are lower and upper 95 % confidence interval.

The results of approximation of the rheological model parameters of the considered materials according to the performed tests are presented in Table 2.

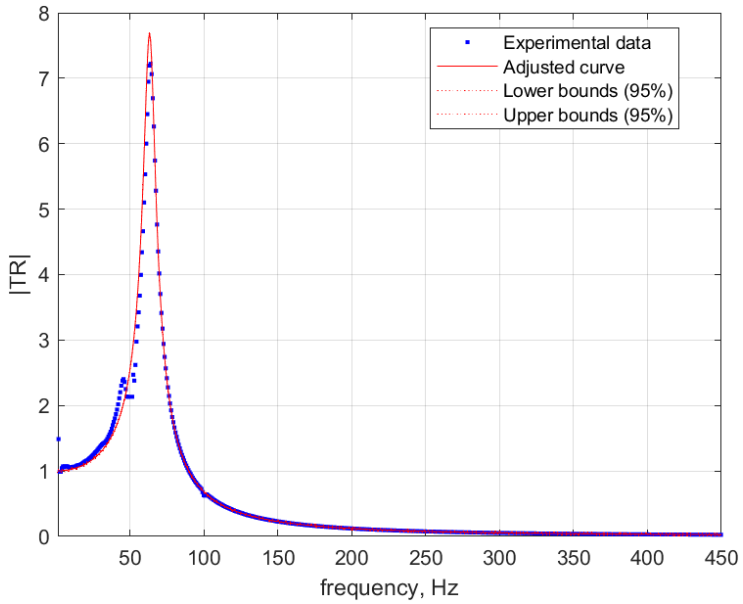

Figure 7. Result of approximation of the transfer function modulus obtained from the results of tests of material type s.2.1 at a load of 2 kPa.

Table 2. Approximation results.

Material identification		Density, kg/m^3	Load, kPa	Approximation results			
				N	γ	τ_ε, s	ω_0, Hz
Materials with different stiffness	Type s.1.1	165	2	288.14	0.83	$8.3791\cdot10^{-9}$	42.64
			5	58.71	0.68	$5.94618\cdot10^{-8}$	24.73
			10	42.86	0.95	$4.82423\cdot10^{-6}$	14.80
	Type s.1.2	190	2	343.73	0.91	$1.09781\cdot10^{-8}$	56.00
			5	19.47	0.73	$1.01912\cdot10^{-6}$	34.01
			10	320.43	0.82	$6.89688\cdot10^{-9}$	22.27
	Type s.1.3	210	2	118.49	0.79	$3.06985\cdot10^{-8}$	54.14
			5	25.03	0.89	$3.28268\cdot10^{-6}$	41.29
			10	56.68	0.85	$4.3767\cdot10^{-7}$	27.43
	Type s.1.4	380	2	38.73	1.00	$1.77606\cdot10^{-6}$	79.69
			5	156.45	1.00	$1.78484\cdot10^{-7}$	53.03
			10	43.95	0.86	$5.2626\cdot10^{-7}$	36.74
	Type s.2.1	350	2	26.84	1.00	$3.14728\cdot10^{-6}$	68.40
			5	17.89	0.88	$2.75135\cdot10^{-6}$	44.99
			10	8.85	1.00	$4.12621\cdot10^{-5}$	31.64

Material identification		Density, kg/m^3	Load, kPa	Approximation results			
				N	γ	τ_ε, s	ω_0, Hz
Materials with different damping	Type d.1.1	343	2	793.082	0.624	$1.659\cdot10^{-6}$	83.21
			5	434.170	0.890	$3.713\cdot10^{-6}$	62.28
			10	101.443	0.920	$1.597\cdot10^{-5}$	45.86
	Type d.1.2	467	2	9334.457	0.639	$4.117\cdot10^{-7}$	80.40
			5	14363.697	0.773	$1.296\cdot10^{-7}$	67.26
			10	15202.664	0.802	$8.908\cdot10^{-8}$	52.42
	Type d.2.1	353	2	18633.192	0.757	$1.865\cdot10^{-7}$	165.39
			5	38750.896	0.678	$1.211\cdot10^{-7}$	130.24
			10	42758.908	0.682	$1.445\cdot10^{-7}$	100.41
	Type d.2.2	572	2	5.861	0.806	$7.042\cdot10^{-4}$	233.32
			5	2849.600	0.544	$1.060\cdot10^{-6}$	193.56
			10	26344.363	0.671	$1.036\cdot10^{-7}$	161.13

Material identification	Density, kg/m³	Load, kPa	Approximation results			
			N	γ	τ_ε, s	ω_0, Hz
Type d.3.1	280	2	266.839	0.588	$1.256 \cdot 10^{-5}$	77.50
		5	4178.858	0.721	$4.445 \cdot 10^{-7}$	63.81
		10	23061.408	0.770	$7.956 \cdot 10^{-8}$	48.46
Type d.3.2	381	2	7520.506	0.487	$4.618 \cdot 10^{-7}$	86.73
		5	6735.431	0.752	$2.565 \cdot 10^{-7}$	74.08
		10	1223.899	0.749	$1.284 \cdot 10^{-6}$	56.31

The scheme for determining the parameters of the rheological material model proposed in this work is shown in the diagram below (Fig. 8).

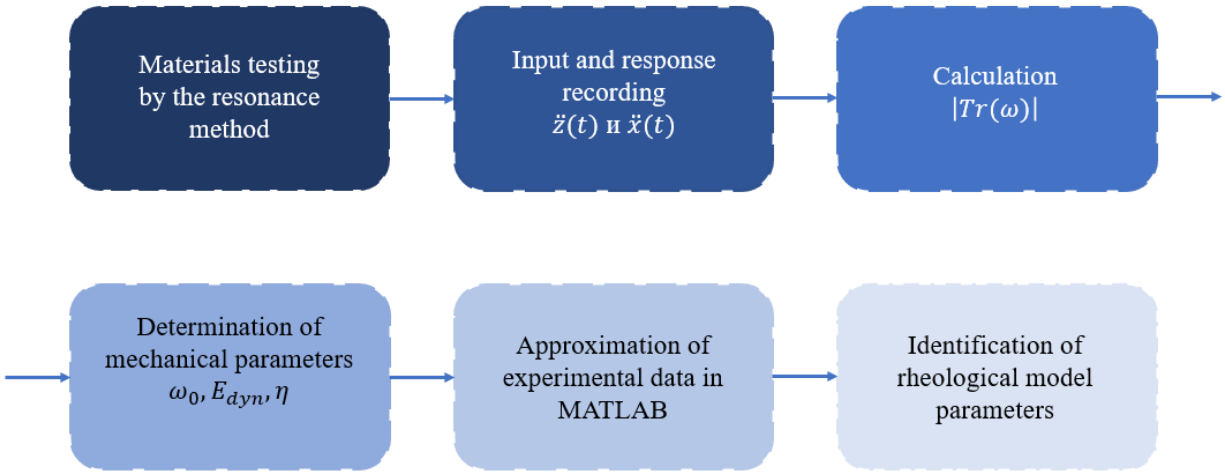

Figure 8. Diagram of identification of parameters of the rheological model of the materials under study.

Let us note several peculiarities of the behavior of the considered vibration-damping materials.

As can be seen from the test results presented in Table 2 and Fig. 9, with increasing load on each of the samples, there is a decrease in the natural frequency of vibrations of the system, which corresponds to the physical concept of the behavior of foamed materials. The increase in the resonance frequency is proportional to the increase in the density of the samples.

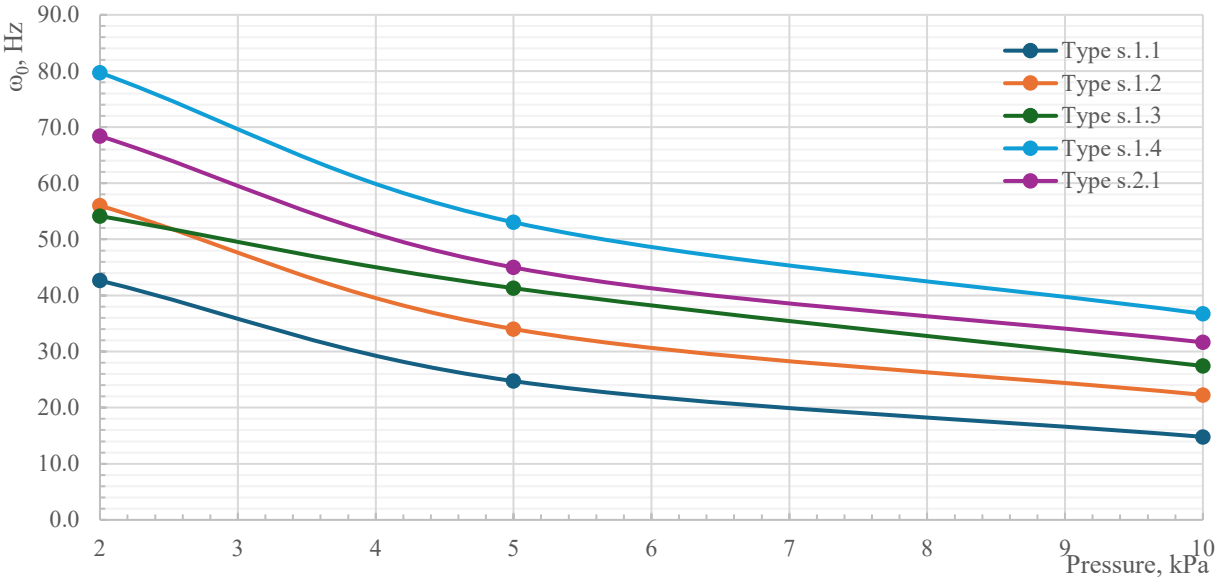

Figure 9. Dependence between natural frequency ω_0 and acting load on the specimen for materials with different stiffness.

The dependence of the fractional parameter on the magnitude of the acting load on the specimen for the tested materials is shown in Fig. 10.

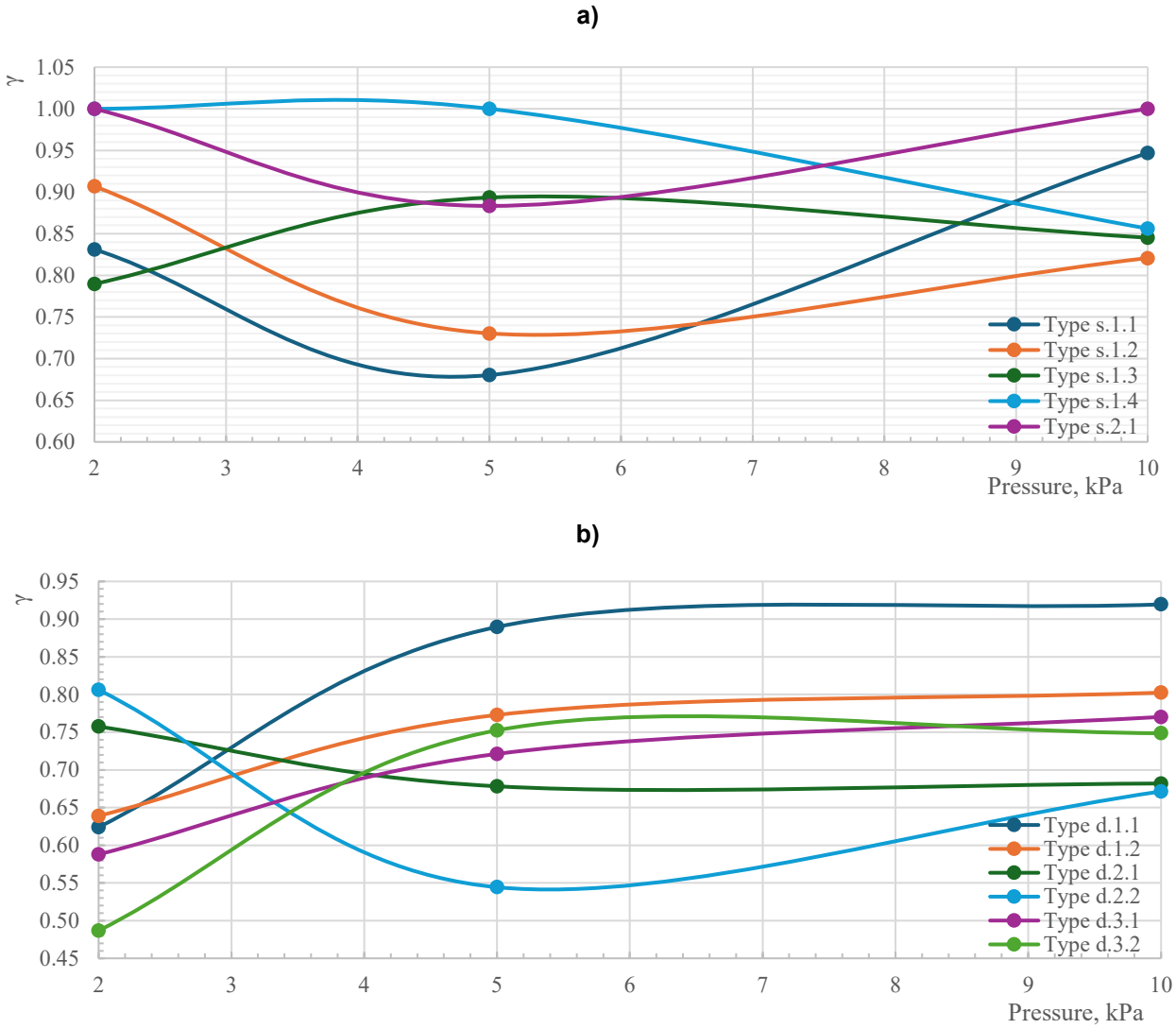

Figure 10. Dependence of the fractional parameter on the sample load: a) for materials with different stiffness, and b) for materials with different damping.

According to the test results, it should be noted that the fractional parameter for all materials is higher than 0.65. This means that the selected materials have predominantly viscous properties.

The nature of the change in the fractional parameter with increasing applied load on the specimen manifests itself in different ways. For example, for soft materials of types s.1.1 and s.1.2 (density 165–190 kg/m^3), the fractional parameter initially decreases from 0.85–0.9 to 0.7–0.75, exhibiting more elastic properties, after which it increases to 0.8–0.95, i.e. the specimen starts behaving more viscous. Samples with higher density – types s.1.3 and s.1.4 (density 210–380 kg/m^3), on the contrary, demonstrate at these values of loads from 2 to 10 kPa a decrease in ductile properties and an increase in elastic ones: the fractional parameter decreases from 0.8–1 to 0.85. That can be related to the change in the structure of the material with combined pores – at compression there is a gradual "collapse" of open communicating pores, pore gas pressure increases, and gas redistribution between internal pores occurs. Gas pumping between the pores is like the work of an ideal viscous damper. Further increases in load and compression strain result in the operation of only closed pores, thus it is worth noting that for denser materials this state is not achieved within the experiment described in Section 2.

The relaxation times determined from the approximation of the experimental data are shown in Fig. 11.

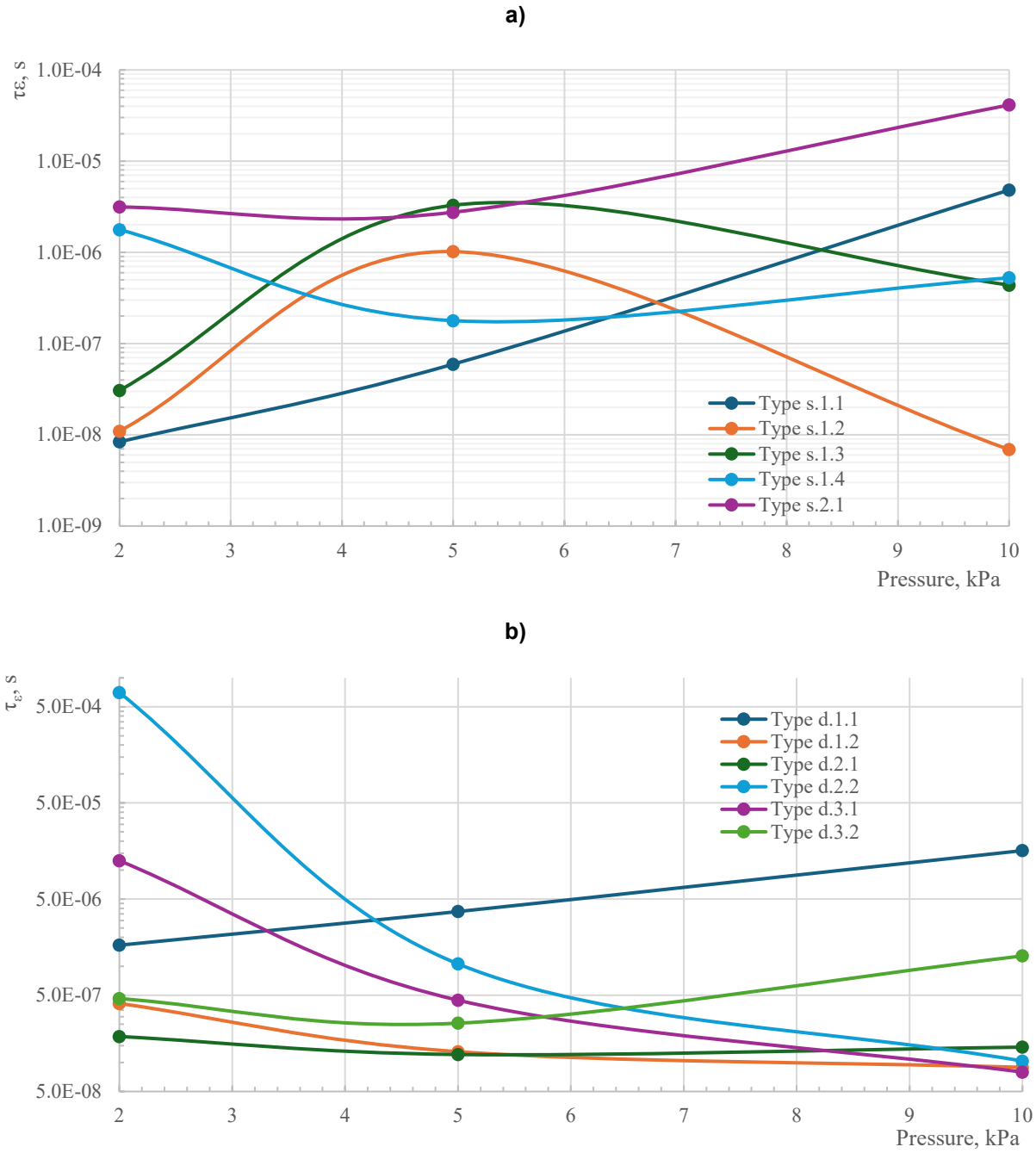

Figure 11. Dependence of relaxation time for samples on load:
a) for materials with different stiffness, and b) for materials with different damping.

It can be noted that the lower the loss coefficient of the material, the shorter will be its relaxation time. At the same time, the relaxation time depends on the acting load on the sample, which is associated with the features of internal damping, including the elasticity of gas in the pores and its pumping between the communicating pores.

The variation of the parameter N, equal to the ratio of creep and relaxation times, depending on the load on the specimen is shown in Fig. 12.

The character of behavior of the parameter N coincides with the character of behavior of the fractional parameter γ. In this case, the more the "viscous" part of the vibration-damping material works, the smaller the parameter N is.

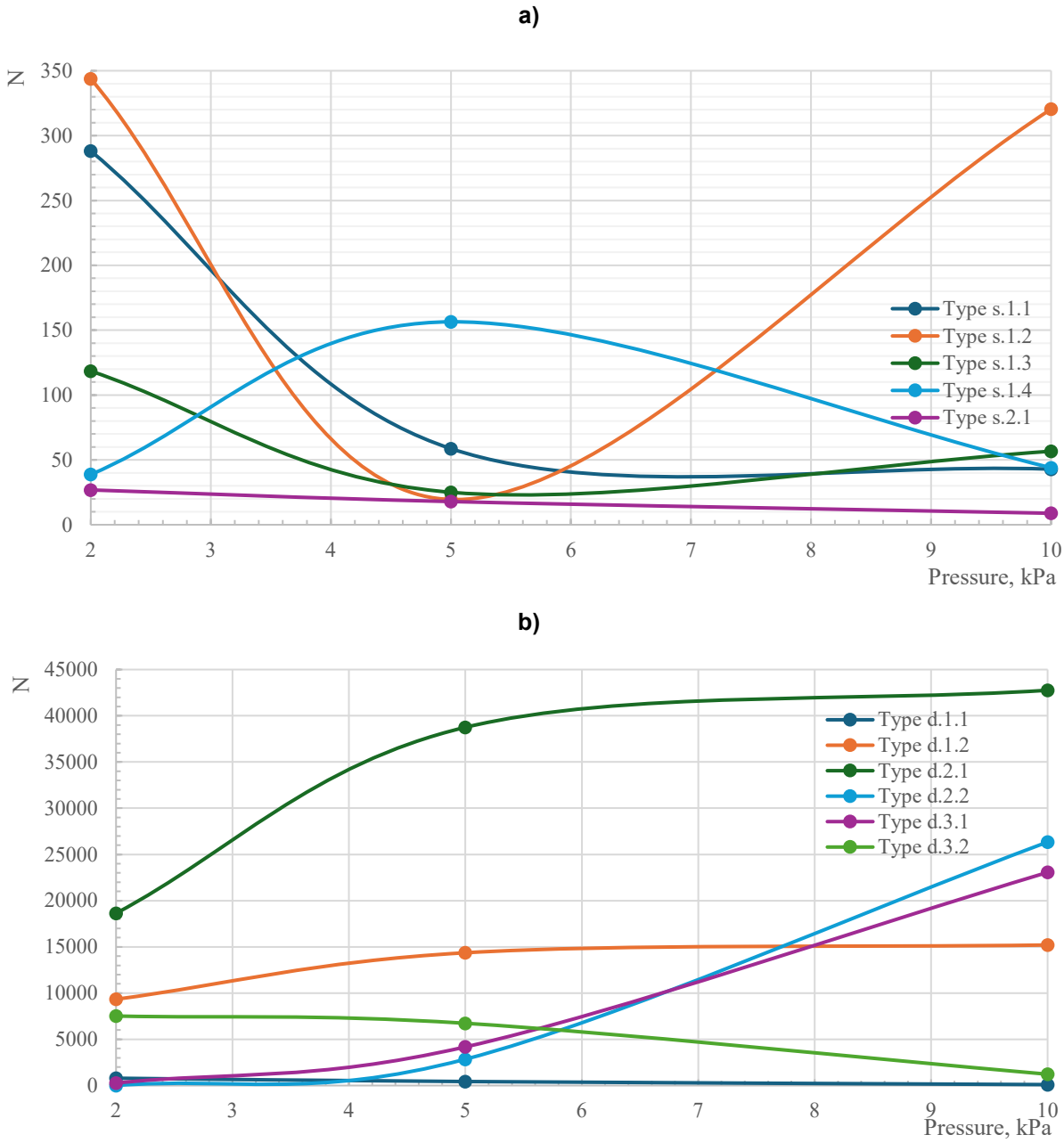

Figure 12. Dependence of the parameter *N* on the sample load: a) for materials with different stiffness, and b) for materials with different damping.

Our findings align with previous research indicating that fractional derivative models effectively capture the viscoelastic behavior of materials with fewer parameters compared to classical models. For instance, a study on solid propellants demonstrated that a three-branch fractional Maxwell model provided a satisfactory agreement with experimental data, highlighting the efficiency of fractional models in describing viscoelastic behaviors [24].

Additionally, the dynamic mechanical analysis of polyurethane foams has been explored in prior studies. One investigation utilized harmonic vibration tests to analyze the dynamic stiffness function of polyurethane foams, revealing insights into their damping effects and frequency response characteristics [25]. Another study emphasized the importance of considering dynamic properties, noting that while static tests are commonly used, the behavior of polyurethane foams under dynamic conditions is crucial for applications such as automotive seating [26].

The simplicity and practicality of the resonance method employed in our study are noteworthy. This approach does not require extensive resources or sophisticated instrumentation, making it accessible for a wide range of applications. The approximation of the experimentally obtained transfer function, with careful selection of initial parameters, resulted in physically meaningful material characteristics.

4. Conclusion

In this paper, we investigated the viscoelastic behavior of foamed polyurethane vibration-damping materials featuring combined porous structures, widely utilized in various engineering and construction applications. To quantify the mechanical characteristics of these materials, dynamic resonance tests were performed, enabling identification of parameters within a FSLS model. The fractional-derivative approach proved highly effective in modeling complex viscoelastic behavior with fewer parameters compared to classical integer-order models.

Our experimental results explicitly demonstrated the significant influence of both material density and pore structure on damping properties:

- For materials with densities ranging from 165 to 380 kg/m^3, an increase in density resulted in higher dynamic moduli of elasticity – from 0.428 MPa to 1.275 MPa (under a load of 5 kPa) – and reduced loss factors from 0.420 to 0.237, indicating a clear inverse relationship between density and damping capacity.
- The pore structure notably influenced damping performance: closed-pore materials exhibited lower loss factors (0.155 at 5 kPa for type s.2.1) compared to open or combined structures, confirming their predominantly elastic behavior.
- The fractional parameter γ, characterizing material viscoelasticity, was found consistently greater than 0.65, confirming predominantly viscous behavior across tested materials. However, γ varied nonlinearly with applied load and density, capturing the transition between elastic-dominated and viscous-dominated behaviors clearly.
- Relaxation times and the parameter N (ratio of creep to relaxation time) also correlated significantly with applied load and material structure, highlighting the complexity of internal damping mechanisms related to gas redistribution among communicating pores.

Overall, our findings emphasize the necessity of fractional-derivative modeling to accurately predict the dynamic behavior of foamed polyurethane materials. The resonance-based testing approach provided reliable data for fractional parameter identification, underscoring its practical applicability without requiring extensive instrumentation. Future research directions should consider broader ranges of material densities and structural variations to further refine fractional models and enhance their predictive capabilities for advanced vibration and seismic isolation applications.

This study contributes significantly to the expanding field of fractional calculus applications in mechanics of viscoelastic materials, bridging theoretical fractional-order models and practical experimental validation. Specifically, the investigation enhances the existing understanding of how fractional-derivative-based rheological models effectively represent complex viscoelastic behavior of foamed polymeric materials used extensively in structural and vibration isolation contexts. Unlike classical integer-order models, fractional-derivative models capture both elastic and viscous responses with greater fidelity while reducing parameter complexity. The quantification and explicit identification of viscoelastic parameters, presented in this research, underscore the pronounced dependency of damping properties on density and pore structure, providing clear quantitative relationships valuable for material selection and system optimization. Furthermore, this study showcases the applicability and robustness of fractional derivative models for accurately predicting dynamic properties, contributing to the advancement of methods that effectively address real-world engineering challenges in vibration and seismic isolation.

References

1. Shitikova, M.V., Krusser, A.I. Models of Viscoelastic Materials: A Review on Historical Development and Formulation. Advanced Structured Materials. 2022. 175. Pp. 285–326. DOI: 10.1007/978-3-031-04548-6_14
2. Rossikhin, Yu.A., Shitikova, M.V. Fractional calculus in structural mechanics. Applications in Engineering, Life and Social Sciences. Part A. 2019. 7. Pp. 159–192. DOI: 10.1515/9783110571905-009
3. Shitikova, M.V. Fractional operator viscoelastic models in dynamic problems of mechanics of solids: a review. Mechanics of Solids. 2022. 57(1). Pp. 1–33. DOI: 10.3103/S0025654422010022
4. Rossikhin, Yu.A., Shitikova, M.V. Application of Fractional Calculus for Analysis of Nonlinear Damped Vibrations of Suspension Bridges. Journal of Engineering Mechanics. 1998. 124(9). Pp. 1029–1036. DOI: 10.1061/(ASCE)0733-9399(1998)124:9(1029)
5. Diethelm, K. Numerical methods for the fractional differential equations of viscoelasticity. Encyclopedia of Continuum Mechanics. Springer. Berlin. Heidelberg, 2020. Pp. 1927–1938. DOI: 10.1007/978-3-662-55771-6_89
6. Kou, L., Bai, Y. Dynamic response of rectangular plates on two-parameter viscoelastic foundation with fractional derivatives. Journal of Vibration and Shock. 2014. 33(8). Pp. 141–147.
7. Hosseinkhani, A., Younesian, D., Farhangdoust, S. Dynamic Analysis of a Plate on the Generalized Foundation with Fractional Damping Subjected to Random Excitation. Mathematical Problems in Engineering. 2018. 2018. Article no. 3908371. DOI: 10.1155/2018/3908371
8. Zhang, C., Zhu, H., Shi, B., Liu, L. Theoretical investigation of interaction between a rectangular plate and fractional viscoelastic foundation. Journal of Rock Mechanics and Geotechnical Engineering. 2014. 6(4). Pp. 373–379. DOI: 10.1016/j.jrmge.2014.04.007

9. Zhu, H.-H., Liu, L., Ye, X. Response of a loaded rectangular plate on fractional derivative viscoelastic foundation. Journal of Basic Science and Engineering. 2011. 19(2). Pp. 271–278. DOI: 10.3969/j.issn.1005-0930.2011.02.011
10. El-Misiery, A.E.M., Ahmed, E. On a fractional model for earthquakes. Applied Mathematics and Computation. 2006. 173(1). Pp. 231–242. DOI: 10.1016/j.amc.2005.10.011
11. Carcione, J.M., Cavalline, F., Mainardi, F., Hanyga, A., Zhang, Z.Z. Time-domain Modeling of Constant-Q Seismic Waves Using Fractional Derivatives. Pure and Applied Geophysics. 2002. 159. Pp. 1719–1736. DOI: 10.1007/s00024-002-8705-z
12. Celauro, C., Fecarotti, C., Pirrotta, A., Collop, A. Experimental validation of a fractional model for creep/recovery testing of asphalt mixtures. Construction and Building Materials. 2012. 36. Pp. 458–466. DOI: 10.1016/j.conbuildmat.2012.04.028
13. Popov, I.I., Shitikova, M.V., Levchenko, A.V., Zhukov, A.D. Experimental identification of the fractional parameter of the fractional derivative standard linear solid model for fiber-reinforced rubber concrete. Mechanics of Advanced Materials and Structures. 2024. 31(17). Pp. 4131–4139. DOI: 10.1080/15376494.2023.2191600
14. Amabili, M. Nonlinear damping in large-amplitude vibrations: modelling and experiments. Nonlinear Dynamics. 2018. 93. Pp. 5–18. DOI: 10.1007/s11071-017-3889-z
15. Alotta, G., Barrera, O., Pegg, E.C. Viscoelastic material models for more accurate polyethylene wear estimation. The Journal of Strain Analysis for Engineering Design. 2018. 53(5). Pp. 302–312. DOI: 10.1177/0309324718765512
16. Ciniello, A.P.D., Bavastri, C.A., Pereira, J.T. Identifying mechanical properties of viscoelastic materials in time domain using the fractional Zener model. Latin American Journal of Solids and Structures. 2016. 14(1). Pp. 131–152. DOI: 10.1590/1679-78252814
17. Shabani, M., Jahani, K., Di Paola, M., Sadeghi, M.H. Frequency domain identification of the fractional Kelvin-Voigt's parameters for viscoelastic materials. Mechanics of Materials. 2019. 137. Article no. 103099. DOI: 10.1016/j.mechmat.2019.103099
18. Amabili, M., Balasubramanian, P., Ferrari, G., Nonlinear vibrations and damping of fractional viscoelastic rectangular plates. Nonlinear Dynamics. 2021. 103(4). Pp. 3581–3609. DOI: 10.1007/s11071-020-05892-0
19. Santos, M. A procedure for the parametric identification of viscoelastic dampers accounting for preload. Journal of the Brazilian Society of Mechanical Sciences and Engineering. 2012. 34(2). Pp. 213–218. DOI: 10.1590/S1678-58782012000200013
20. Beda, T., Chevalier, Y. New Methods for Identifying Rheological Parameter for Fractional Derivative Modeling of Viscoelastic Behavior. Mechanics of Time-Dependent Materials. 2004. 8. Pp. 105–118. DOI: 10.1023/B:MTDM.0000027671.75739.10
21. Espíndola, R.L., Silva Neto, J.L., Lopes, F.J. A generalized fractional derivative approach to viscoelastic material properties measurement. Applied Mathematics and Computation. 2005. 164(2). Pp. 493–506. DOI: 10.1016/j.amc.2004.06.099
22. Guo, X., Yan, G., Benyahia, L., Sahraoui, S. Fitting stress relaxation experiments with fractional Zener model to predict high frequency moduli of polymeric acoustic foams. Mechanics of Time-Dependent Materials. 2016. 20(4). Pp. 523–533. DOI: 10.1007/s11043-016-9310-3
23. Nashif, A.D., Jones, D.I.G., Henderson, J.P. Vibration Damping. Wiley-Interscience. New York, 1985. 480 p.
24. Fang, C., Shen, X., He, K., Yin, C., Li, S., Chen, X., Sun, H. Application of fractional calculus methods to viscoelastic behaviours of solid propellants. Philosophical Transactions of the Royal Society A. 2020. 378(2172). Article no. 20190291. DOI: 10.1098/rsta.2019.0291
25. Duboeuf, O., Dupuis, R., Aubry, E., Lauth, M. Harmonic Vibration Test for the Analysis of the Dynamic Behaviour of Polyurethane Foams. Dynamic Behavior of Materials. 1. Springer. Cham, 2016. Pp. 61–67. DOI: 10.1007/978-3-319-22452-7_10
26. Dossi, M., Moesen, M., Brennan, M., Vandenbroeck, J. Dynamic Comfort and Vibration Damping with Polyurethane Foams. 2016 Polyurethanes Technical Conference. Baltimore, 2016. Pp. 60–73.

Information about the authors:

***Marina Shitikova**, Doctor of Physics and Mathematics*
ORCID: https://orcid.org/0000-0003-2186-1881
E-mail: shitikova@vmail.ru

***Vladimir Smirnov**, PhD in Technical Sciences*
ORCID: https://orcid.org/0000-0001-5679-9542
E-mail: SmirnovVA@mgsu.ru

Received 17.01.2025. Approved after reviewing 11.03.2025. Accepted 15.03.2025.